Comparison of low-frequency data from co-located receivers using frequency dependent least-squares-subtraction scalars

Kevin W. Hall, Gary F. Margrave and Malcolm B. Bertram

ABSTRACT

Eight-trace shot gathers were created from a subset of the data collected during the Priddis low-frequency comparison test. For this study, we are only considering the 2-10 Hz EnviroVibe shots. The geophone data were decimated to a ten meter spacing to match the other datasets. The southernmost receiver station was dropped from the geophone and accelerometer data, as there was no seismometer to compare to for this station. Sixty seconds of seismometer data were extracted from the continuous data stream based on time of shot, de-biased to remove the resulting (sometimes large) zero Hz component, and re-sampled from 10 ms to 2 ms to match the other data. The resulting datasets were aligned based on cross-correlations, and then compared by filtering the traces with a 1 Hz wide sliding bandpass filter (0.1 Hz increment from 2-10 Hz), and calculating a least-squares-subtraction scalar (LSSS) for each bandpass filter step. In general, the integrated Sercel 428XL/DSU3 data is closest in overall amplitude to the raw Nanometrics/Trillium seismometer data. The Aries/geophone and Ion/VectorSeis data are roughly 10^8 times smaller than the seismometer data in amplitude. The LSSS depend on amplitude, frequency, phase, source-receiver offset, and quality of sensor placement in or on the ground.

INTRODUCTION

The 2009 Priddis seismometer test survey is described by Bertram et al. (2009), and are also analyzed by Eaton et al. (2009). Figure 1 shows a detailed schematic of the survey layout in the field. Four recording systems were used (Table 1). Seismometers and 3C geophones were oriented inline, accelerometers were aligned to magnetic north. For this report, we are disregarding data collected from the weight-drop source and for all 2-100 Hz vibe sweeps (Table 2). The 2-100 Hz sweeps are being excluded, at least initially, due to the fact that the seismometers have a maximum sample rate of 10 ms, which yields a Nyquist frequency of 50 Hz. The mono-frequency 3 and 5 Hz sweeps were used for testing code, but not for analysis. As the EnviroVibe is not designed to operate below eight Hertz, the sweeps were done at 10% of maximum force, and many phase errors were observed in the field. Since we are looking at uncorrelated data, this is not expected to be a factor.

It turns out that we cannot use the unmodified raw data for two main reasons: 1) while three of the recording systems sampled the wavefield at a two millisecond sample rate, the seismometer data were sampled at ten milliseconds, and 2) the data do not have a precise time-zero for each shot. The seismometers synchronize with GPS time, and the system clocks of the other recorders were manually synchronized to GPS time. This means that there could be up to one second of error in the time of shot when comparing between the different systems. In addition, there is no time-break available for the seismometer (no trigger recorded) or DSU3 data, as the Sercel system was manually triggered prior to each shot.

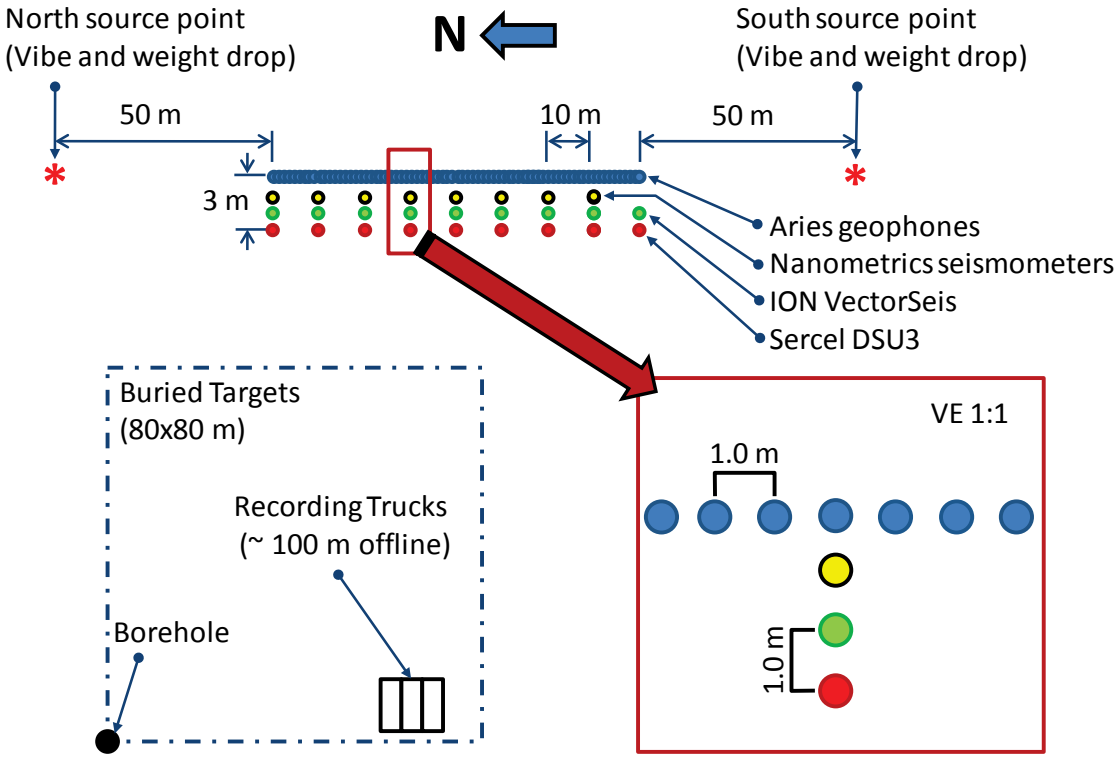

FIG. 1. Schematic of survey layout at the Priddis test site.

Table 1. Recording system low-cut filters

Operator/Recording system/Sensor	Recording system	Sensor	Low-cut filter
University of Calgary	Aries	10 Hz 3C geophones	1 Hz
Ion	Scorpion	VectorSeis	1.46 Hz
CGGVeritas	Sercel 428XL	DSU3	None
University of Calgary	Nanometrics Trillium	Broad-band seismometer	0.004 Hz

Table 2. List of data used for this report. Weight-drop source and 2-100 Hz sweeps are omitted.

ARAM FFID	Description
39-40	North VP, 2-10 Hz, 50 s, 25 s start taper, 0.1 s end taper
45-50	North VP, 2-10 Hz, 30 s, 15 s start taper, 0.1 s end taper
51-54	North VP, 2-10 Hz, 10 s, 5 s start taper, 0.1 s end taper
55-58	North VP, 5 Hz mono, 30 s, 0.1 s start/end taper
59-62	North VP, 3 Hz mono, 30 s, 0.1 s start/end taper
71-72	South VP p, 2-10 Hz, 50 s, 25 s start taper, 0.1 s end taper
73-74	South VP, 2-10 Hz, 30 s, 15 s start taper, 0.1 s end taper
75-76	South VP, 2-10 Hz, 10 s, 5 s start taper, 0.1 s end taper
77-78	South VP, 5 Hz mono, 30 s, 0.1 s start/end taper
79-80	South VP, 3 Hz mono, 30 s, 0.1 s start/end taper

LEAST-SQUARES-SUBTRACTION SCALARS (LSSS)

The amplitudes of any two data traces (S_1 and S_2), can be matched by multiplying one of the traces by some constant, a. The best-fit constant can be determined in a least-squares-subtraction sense by defining some number

$$\varepsilon = \sum_k (S_{1k} - aS_{2k})^2, \tag{1}$$

where k represents individual samples within each data trace. Differentiating ε with respect to a and requiring that the result equal zero gives

$$\frac{1}{2}\frac{\partial \varepsilon}{\partial a} = \sum_k S_{1k}S_{2k} - a\sum_k S_{2k}^2 = 0, \tag{2}$$

which can then be solved for

$$a = \frac{\sum_k S_{1k}S_{2k}}{\sum_k S_{2k}^2}, \tag{3}$$

where equation (3) is equivalent to the zero-lag cross-correlation divided by the zero-lag auto-correlation.

In order to investigate amplitude dependence on frequency, the input traces are narrow-pass filtered before calculating the LSSS. For this report, input traces were filtered with a series of 1 Hz wide bandpass filters from 2-10 Hz in 0.1 Hz increments.

So, for subsequent figures, the LSSS plotted at 2 Hz will be the result from equation (3) for input traces filtered with a 1.5-2.5 Hz pass-band.

Testing using synthetic 2-10 Hz sweeps in Matlab shows that if trace S_1 equals trace S_2*2, the LSS scalar will be 2 for all frequencies. If $S_1 = S_2$*0.5, the answer will be 0.5 for all frequencies. If $S_1 = S_2$ the answer will be 1, but, if we time-shift S_2 relative to S_1 the answer varies from +1 to -1 for a synthetic mono-frequency sweep (not shown), and between +1 and -0.8 for our synthetic 2-10 Hz sweep (Figure 2).

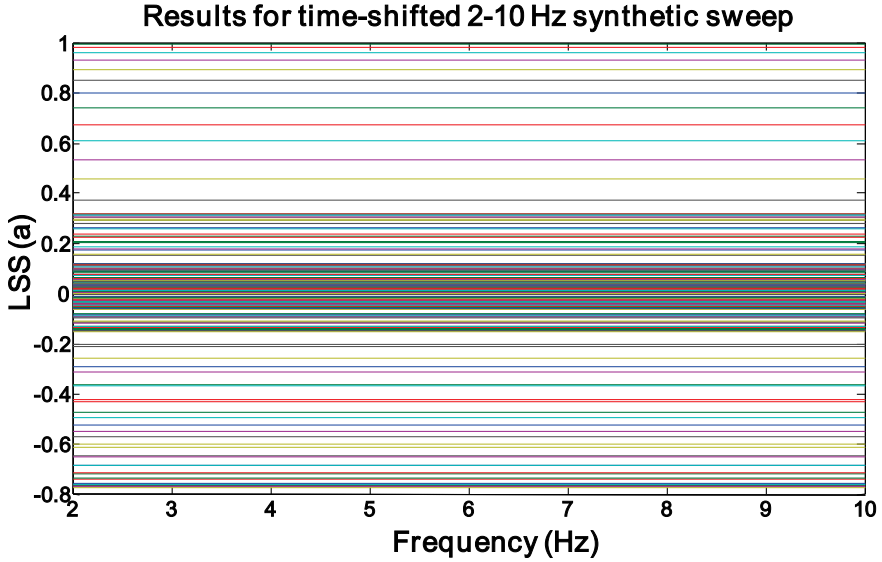

FIG. 2. Frequency dependent LSSS results for a synthetic 2-10 Hz sweep compared to multiple time-shifted copies (one sample shift per calculation for one 2 Hz cycle).

DATA PREPARATION

Figure 3 shows the processing flow used to calculate frequency dependent LSSS. Matlab was used to extract sixty seconds of seismometer data from the continuous data stream using a start time based on time of Aries shot from the Aries observer's notes. Source gathers were then created for each component (east, north and vertical) and written to SEG-Y. GEDCO Vista was then used to combine and sort the data for the four receiver types. The data were coarsely aligned to a zero time that was arbitrarily set to 100 ms. The seismometer data were de-biased and re-sampled to a two ms sample rate to match the other datasets. De-biasing is required since low frequency components (less than one Hertz) in the seismometer data were truncated when the sixty second records were extracted, resulting in an apparent DC bias. Accelerometer data were integrated to obtain velocity curves. The sorted and combined datasets (vertical, inline, crossline) were written to SEG-Y for further processing in Matlab. No component rotations have been performed for this initial work.

Figure 4 shows the combined dataset with traces individually RMS scaled for display. Note that at this scale, the character of the uncorrelated data is clearly different for the north versus the south vibe point. This appearance carries through to the amplitude spectra (Figure 5; RMS scaled for display). Interestingly, there are no obvious differences

between the amplitude spectra for the 10, 30 and 50 s long 2-10 Hz sweeps. There is a peak at 5 Hz for the 5 Hz sweep, and harmonics at 10, 15, 20 Hz, etc. There is no visible peak for the 3 Hz mono-frequency sweep at this scale, but 9 Hz and higher harmonics can be seen. Both mono-frequency sweeps show a prominent peak at the 15 Hz harmonic. For the 2-10 Hz sweeps, most of the amplitude content appears between 15 and 35 Hz, and is likely due to recorder generators and source noise.

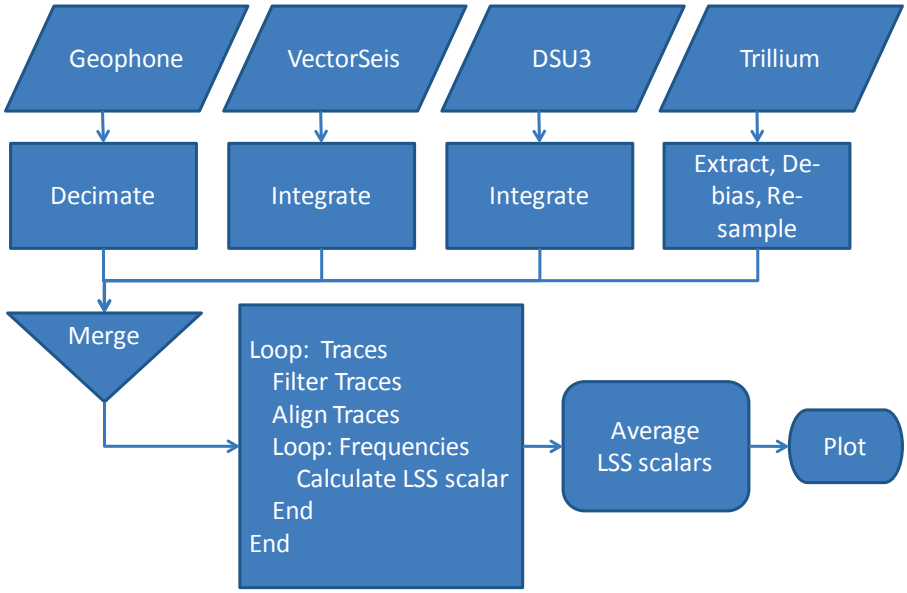

FIG. 3. Processing Flow.

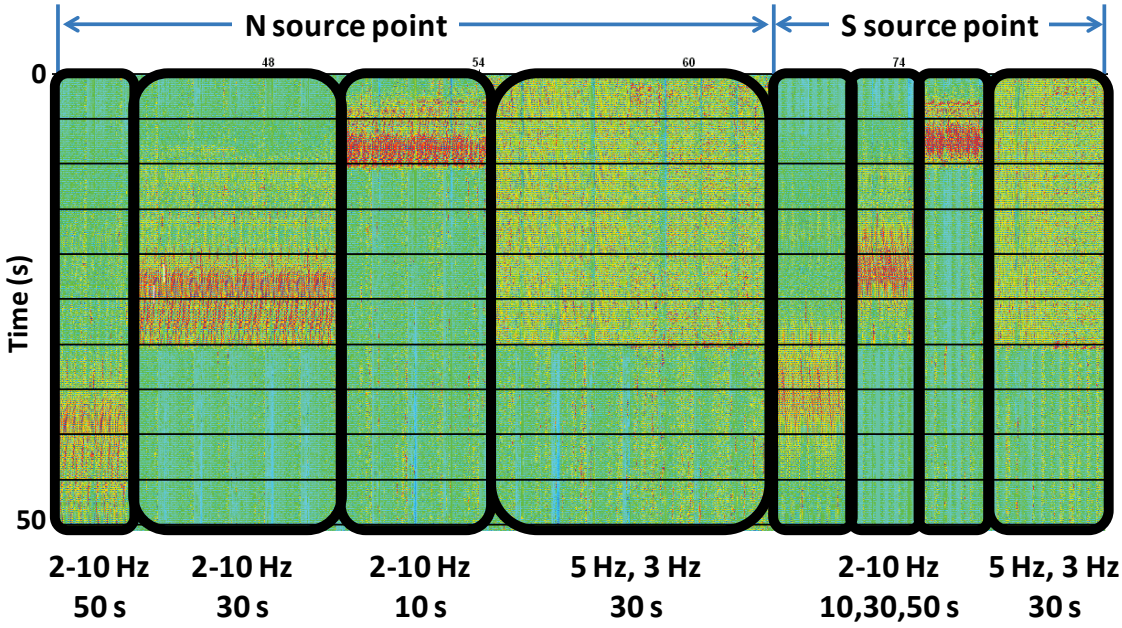

FIG. 4. Display of all vertical component Mini-Vibe uncorrelated data (sensors interleaved) used for this report. Traces are individually RMS scaled for display.

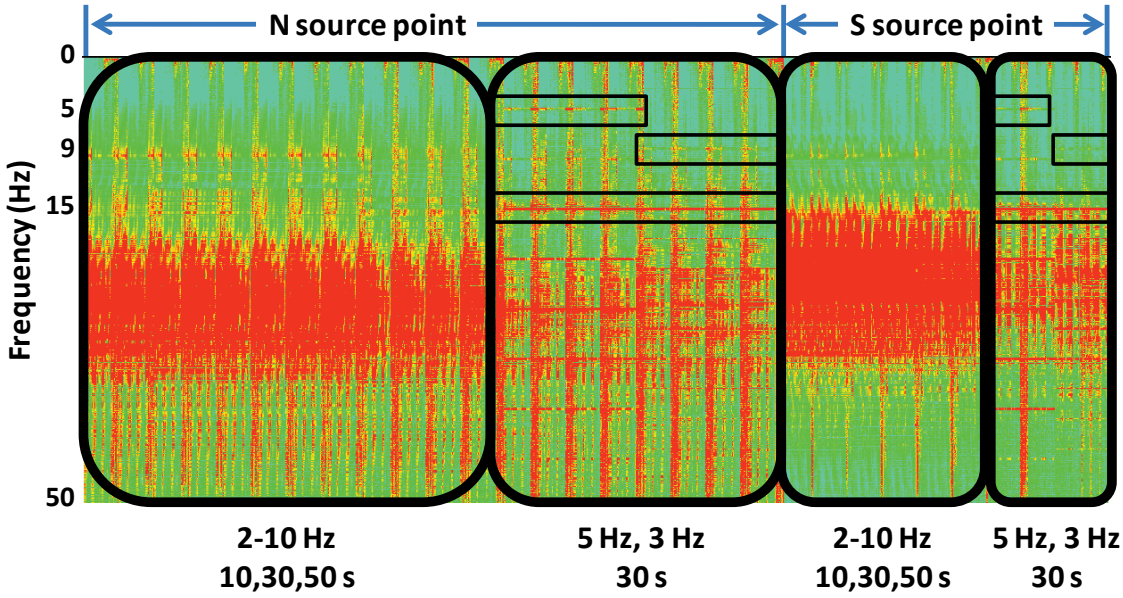

FIG. 5. Amplitude spectra for Figure 2, spectra are individually RMS scaled for display.

Data alignment

The geophone and accelerometer data were filtered (2-10 Hz) and aligned to the seismometer traces station by station using 'filtf,' 'maxcorr' modified to return the maximum positive correlation rather than the maximum correlation, and 'stat' to sub-sample time-shift the traces (eg. Figure 6). 'Sectfilt,' 'maxcorr,' and 'stat' are available in the CREWES Matlab toolbox. The data compare well visually, but minor differences can be seen throughout the sweep. The seismometer response at the end of the sweep is larger in amplitude than any of the other sensors.

Least-squares-subtraction scalar results for real data

Figure 7 shows the LSSS calculated for the traces shown in Figure 6, and Figure 8 shows the LSSS calculated for all of the 2-10 Hz data for the North VP (data shown in Figure 4). The dashed lines in Figure 8 have the same slope, and highlight a source-receiver offset dependence of the LSSS. The data for the South VP show an opposite slope (not shown). Black rectangles show a LSSS anomaly at receiver station 5 (90 m from the northern VP). It can be clearly seen on the geophone and VectorSeis comparisons, but is less clear on the DSU3 plot.

Figure 9 shows the LSSS curves for all 2-10 Hz sweeps (north and south VP's). This is essentially a sideways view of Figure 8. Disregarding any offset effects, the average curves for these LSSS data are shown in Figure 10, which looks very similar to the result from a single trace (eg. Figure 7).

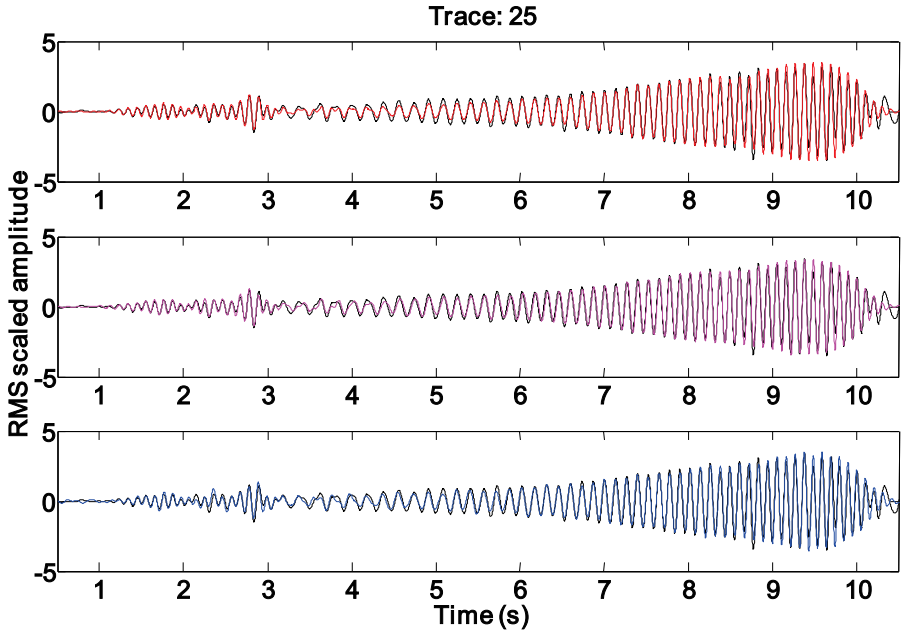

FIG. 6. Aligned traces from the northernmost receiver station (vertical component, uncorrelated) for Aries FFID 54 (North VP, 2-10 Hz 10 s sweep). Red is the geophone data; Magenta is the integrated VectorSeis data; Blue is the integrated DSU3 data; Black is the seismometer data (repeated three times). All traces are 2-10 Hz bandpass filtered for trace alignment and display.

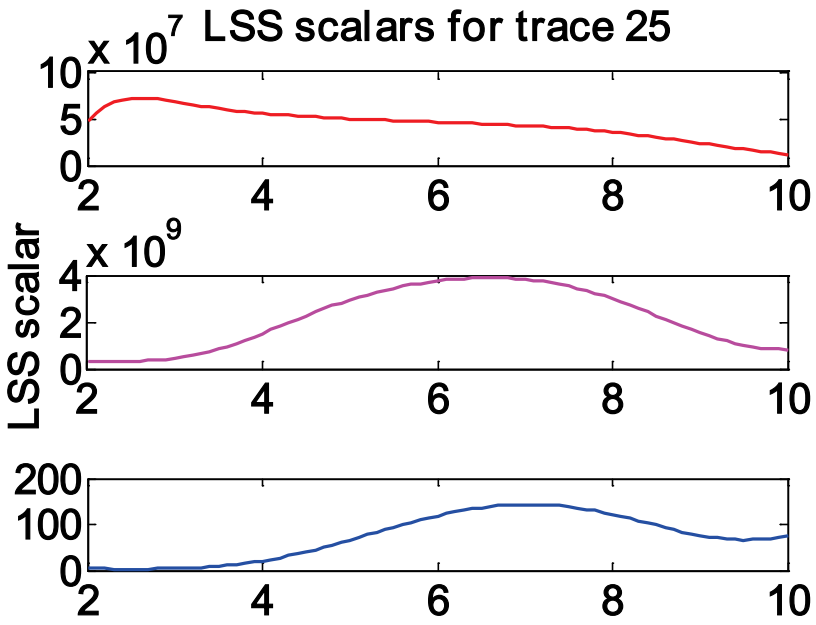

FIG. 7. Frequency dependent least-squares-subtraction scalars for unscaled trace 25 (scaled traces shown in Figure 6). Red line is the geophone data; Magenta line is the integrated VectorSeis data; Blue line is the integrated DSU3 data.

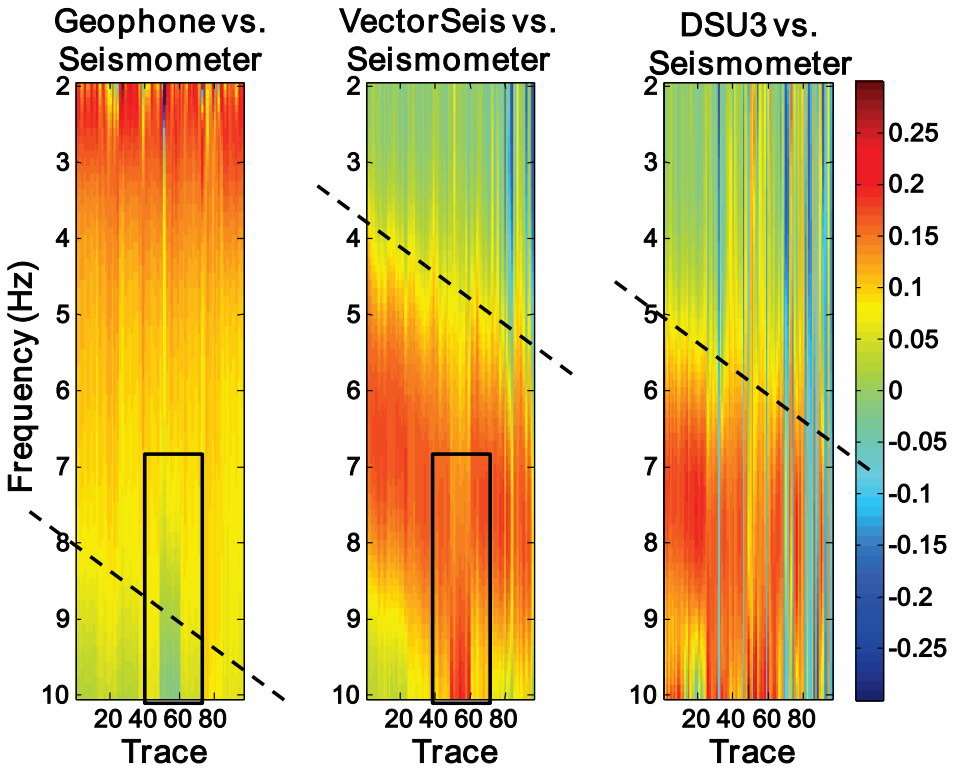

FIG. 8. LSSS for all 2-10 Hz sweeps at the northern VP, normalized for display. Dashed lines (same slope) show a LSSS dependence on source-receiver offset for all sensors. Black rectangles highlight an LSSS anomaly at station 5.

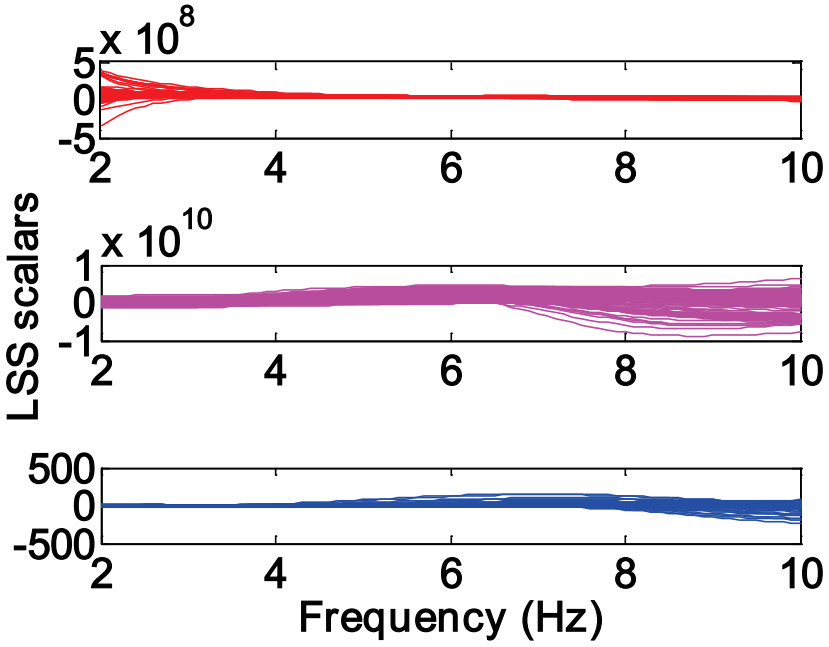

FIG. 9. LSS scalars for all 2-10 Hz sweeps (N and S VP's). Red lines are for geophone data; Magenta lines are for integrated VectorSeis data; Blue lines are for integrated DSU3 data.

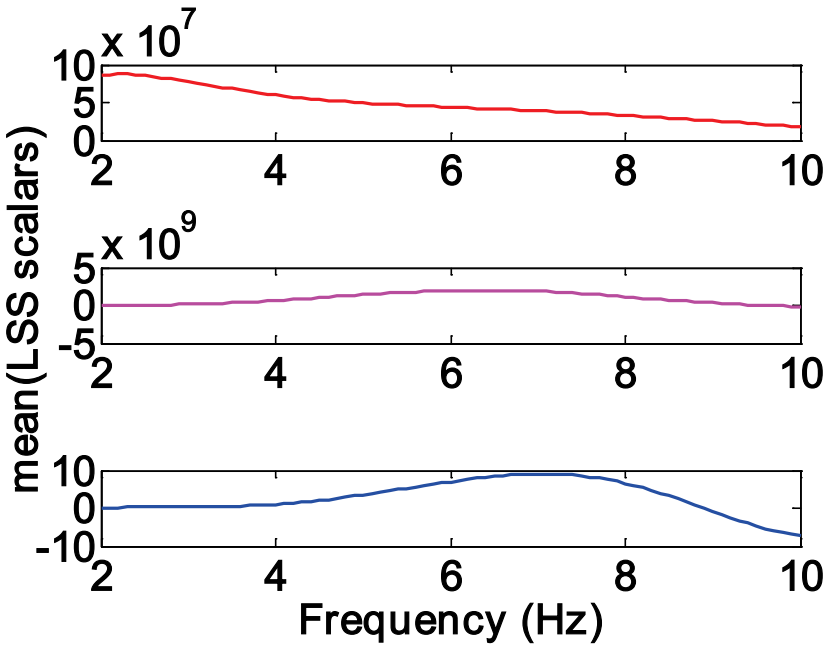

FIG. 10. Averaged least-squares-subtraction scalars for all sensors, all 2-10 Hz sweeps. Red lines are the geophone data; Magenta lines are the integrated VectorSeis data; Blue lines are the integrated DSU3 data.

DISCUSSION

The least-squares-subtraction scalar has been shown to depend on amplitude and phase in synthetic data. Real data results show that the LSSS is frequency dependent (Figure 8-10). The results for station 5 of the real data show that it also depends on the quality of sensor placement in or on the ground (black rectangles; Figure 8). The LSSS anomaly at station 5 can be clearly seen on the geophone, integrated Vectorseis and integrated DSU3 LSSS curves, implying that the seismometer placement at station 5 was somehow different than at adjacent stations. Finally, the dashed lines in Figure 5 highlight source-receiver offset dependent effects in the LSSS.

The geophone data amplitudes are 10^7 times smaller than the seismometer amplitudes, and the Vectorseis data are similar, at 10^9 times smaller. The DSU3 amplitudes are closest to the raw seismometer amplitudes. If instrument response was identical, or merely scaled in amplitude, the LSSS curves should be horizontal lines. The fact that they are not may be explained by the observation that filtering with a 2-10 Hz pass-band before aligning the traces gives a different LSSS result than filtering with a 2-40 Hz pass-band, or not filtering at all. This suggests that we may need to examine trace alignment after applying the narrow-pass filters, and possibly consider doing the trace alignment after the filter. Performing the calculations in this manner would take considerably more computation time.

The geophone versus seismometer LSSS curve looks quite different than the accelerometer curves. The general decrease in geophone amplitude towards lower frequencies relative to the seismometer data (increase in LSSS curve; Figures 7 and 10) is

likely due to our narrow-pass filters starting to see the low-cut filter in the Aries recording system.

The Vectorseis and DSU3 versus seismometer LSSS curves are quite similar to each other, disregarding scale. These data appear to match the seismometer data best below 4 Hertz, and less well at higher frequencies. Again, this result could be due to issues with trace alignment after narrow-pass filtering.

The fact that the VectorSeis and DSU3 LSSS curves are similar to each other, but different to the geophone result shows that the LSSS can be used to conduct sensor comparisons.

FUTURE WORK

We need to do more work to confirm, and refine these initial results. We also need to examine the inline and crossline components of this dataset, as well as the weight-drop and 2-100 Hz sweep data.

ACKNOWLEDGEMENTS

We would like to thank the field crew, which included CREWES faculty, staff and students, as well as Kris Dash from ARAM Systems, Tom Preusser and Aaron Kennedy from CGGVeritas (Sercel/DSU3), Brett Frederickson from ION (Scorpion/Vectorseis), and Waled Bin Merdhah from ERCB/Alberta Geological Survey (Nanometrics/Trillium). We would also like to thank Dave Eaton for allowing the use of his seismometers for this experiment.

REFERENCES

Bertram, M.B., Hall, K.W., Margrave, G.F., Lawton, D.C., Wong, J., Gallant, E.V., 2009, Seismic acquisition projects 2009: Crewes Research Report: **21**.

Eaton, D.W., Pidlisecky, A., Ferguson, R.J., Hall, K.W., 2009, Absolute strain determination from a calibrated seismic field experiment: Crewes Research Report, **21**.